CHAPTER II
LITERATURE REVIEW

2.1 Hydrogen Storage Target

Hydrogen storage is an important topic to the hydrogen economy, particularly, storing hydrogen for vehicular applications or the fuel cell driven cars. The requirement of a hydrogen storage system for practical applications in both economic and environmental reasons including (Grochala and Edwards, 2004):

1) High storage capacity in both gravimetric and volumetric density.
2) Operating temperature in the range of 60–100 °C, suitable for PEM (proton exchange membrane) fuel cell applications
3) Quick charging and recharging hydrogen
4) Low cost
5) Safe and reasonable cost

The hydrogen storage targets, which are fixed by the U.S. department of energy (DOE) for driving a car more than 500 km, are shown in Table 2.1.

Table 2.1 Targets of the U.S. DOE hydrogen storage system targets (Satyapal *et al.*, 2007)

Storage parameter	Units	2010	2015
System gravimetric capacity (Specific energy)	H_2/kg system	0.060	0.090
System volumetric capacity (Energy density)	H_2/L system	0.045	0.081
Storage System cost	\$/L H_2	133	67
Life time charge-recharge cycle	Cycles	1000	1500
Operating temperature	°C	-40/85	-40/85
Refueling rate	kg H_2/min	1.5	2.0

The DOE on-board hydrogen storage system performance targets were developed through Freedom CAR, a partnership between DOE and the U.S. Council for Automotive Research. The performance targets developed are system and application driven, based on achieving similar performance and cost levels as current gasoline fuel storage systems for light-duty vehicles. The storage system includes the tank, valves, regulators, piping, mounting brackets, insulation, added cooling capacity, thermal management, and any other balance-of-plant components in addition to the first charge of hydrogen and any storage media such as solid adsorbent or liquid used to store the hydrogen (Satyapal *et al.*, 2007).

The technical challenge in identifying an ideal hydrogen storage system is to meet simultaneously all the targets for practical on-board vehicular applications are shown in Figure 2.1.

These targets or required properties are closely associated with three sets of parameters: structure (crystalline form, specific surface area or particle size, and structural defects), chemistry (components, composition, phases, catalysts, and impurities), and reaction or diffusion path (elementary reactions, transient species, etc.). These are interacting, and the critical issues differ for different types of hydrogen storage materials (Guo *et al.*, 2008).

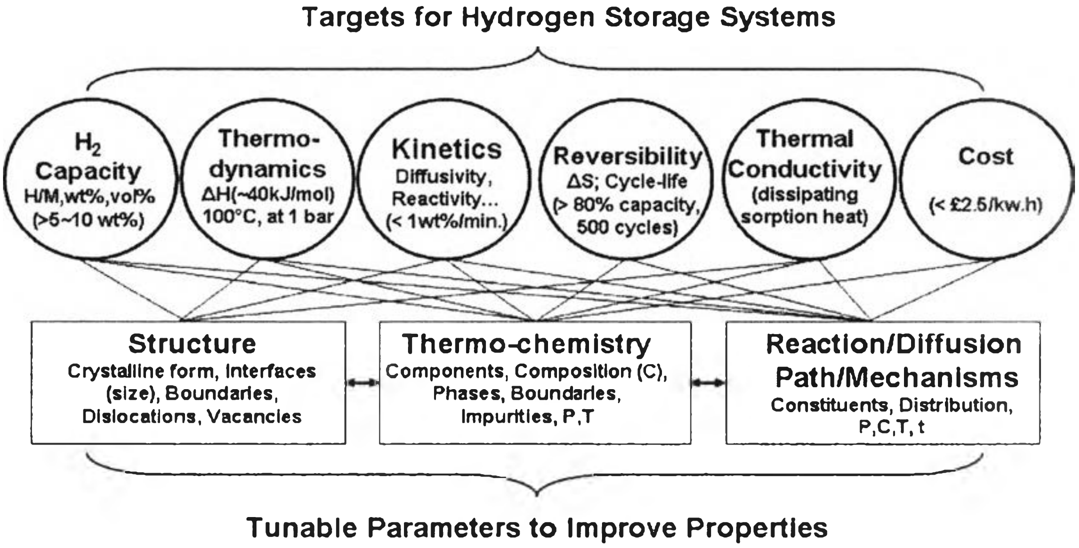

Figure 2.1 Practical targets for on-board hydrogen storage in relation to key materials parameters (Guo *et al.*, 2008).

2.2 Properties of Material-based Hydrogen Storage Media

Hydrogen storage media can be subdivided into four distinct categories: (1) high pressure storage, (2) metal hydrides, (3) adsorption of hydrogen, and (4) chemical hydrogen storage. The scope of the properties of storage media appears to be relevant for near-term PEM fuel cell and non-automotive fuel cell markets including the importance of reliable material property measurement techniques to facilitate the development of hydrogen storage materials. The hydrogen storage properties of a material can be significantly influenced by not only individual sample characteristics including chemical composition and distribution, micro- and macro-scopic material structure, and etc., but also pressure, temperature, and sample size.

The following information provides a general description of the materials properties along with several examples of recent advancements in hydrogen storage materials that will clearly impact system design for near-term fuel cell markets (McWhorter *et al.*, 2011).

2.2.1 Capacity

For hydrogen storage materials, capacity is defined as the amount of hydrogen stored per unit weight (gravimetric capacity) or volume (volumetric capacity), which is often expressed in terms of the chemical energy of stored hydrogen. Capacity is commonly represented as a materials- or system-based value, where it is characterized as the ratio of hydrogen mass stored to the mass or volume of total material or material plus the balance of plant (BOP system) components. The main difference in the two values lies in the fact that the system-based capacity is an upper limit to the amount of useable hydrogen and the materials based value is a measure of the absolute capacity, not accounting for any ancillary fuel system components such as the material containment vessel, piping, and pressure regulators.

Adsorbent or sorbent systems have demonstrated high surface area materials capable of achieving reasonable storage capacities. For example, a metal-organic framework material (MOF) like MOF-5 has exhibited hydrogen capacity about 7.1 wt% at -196 °C and 4 MPa (McWhorter *et al.*, 2011).

2.2.2 Thermodynamics

Hydrogen can be stored in materials dominated by several different bonding mechanisms that require a fundamental understanding of the thermodynamic properties of the hydrogen–material interaction. The thermodynamic properties determine the equilibrium relationship between the operating temperature and pressure, and therefore influence several practical operational parameters of the hydrogen storage system such as charge/discharge heat transfer requirements and available pressure of desorbed/discharged hydrogen.

From a thermodynamics perspective, an optimum material would be reversible and desorb hydrogen near room temperature at a sufficient rate to power the fuel cell system while maintaining an equilibrium hydrogen pressure of at least 0.1 MPa. Also, the material would have rehydrogenation/refill kinetics to allow system recharge (McWhorter *et al.*, 2011).

For practical applications, rapid hydrogen desorption is required around 100 °C and one atmospheric pressure, which corresponds to an enthalpy of formation around 15–25 kJ/mol H_2. Hence, an ideal hydrogen storage system is likely to involve hybrid sorption mechanisms and/or reaction paths that can result in an effective enthalpy change lower than that of simple chemisorption but much higher than that of physisorption. Designs from electronic structures offer the possibility of identifying some promising candidates.

Most chemical hydrogen storage materials, both with exothermic and endothermic hydrogen release are not readily reversible via direct hydrogenation but the material can be regenerated with other chemical reactions and can be achieved by following multi-step/different reaction paths in the case of reactive hydrogen sorption between two or more species (Guo *et al.*, 2008).

2.2.3 Reversibility

Thermodynamic reversibility is an ideal concept, where a process is said to be “reversible” if it can be reversed by infinitesimal changes of a property without causing any loss or dissipation of energy, i.e. the total entropy change is zero. In theory, all processes are reversible. In practice, good reversibility is only obtained if comparable forward and reverse reactions fall well within practically achievable conditions, e.g. temperature, pressure, and kinetics. This effectively means that the rate-controlling energy barriers for the forward and reverse processes (reactions) should be relatively small and of similar values (Guo *et al.*, 2008).

2.2.4 Kinetics

Understanding the kinetics of hydrogen storage materials involves measuring and understanding the rate and mechanism(s) involved in hydrogen uptake and release. The mechanisms are comprised of various dynamic processes, such as surface interactions, mass transport phenomena, and nucleation, any of which could act as the rate limiting step(s) or kinetic barrier(s). From a practical standpoint the fuel system kinetics determine the rate, at which a material can supply hydrogen to a fuel cell to maintain a desired power load or conversely, the rate, at which a material can be refueled (McWhorter *et al.*, 2011).

Hydrogen desorption actually involves multi-steps: de-bonding from host atoms, diffusion in a host structure, diffusion to/along surfaces, formation of hydrogen molecules, and dissociation from the surface of the material (the reverse occurs in absorption). The slowest step determines the overall kinetics of sorption. It is usually difficult but important to pin point which step is rate controlling in hydrogen sorption (Guo *et al.*, 2008).

Each class of hydrogen storage material has its own set of unique kinetic barriers, which can be a significant factor when selecting these materials for hydrogen storage. Although kinetic barriers exist among all storage materials, there are some materials that could meet the kinetic requirements for operation of a PEM fuel cell. Furthermore, recent discoveries in nanoconfinement of hydride materials could prove effective in reducing kinetic barriers for several other classes of materials (McWhorter *et al.*, 2011).

2.2.5 Thermal Conductivity

For hydrogen storage, the desorption reaction is usually endothermic and absorption exothermic. This means that considerable amount of reaction heat needs to be dissipated during hydrogen charging (absorption) and heating is needed for hydrogen desorption. Highly conductive cooling/heating structures are necessary in the design of a hydrogen storage system (Guo *et al.*, 2008).

2.2.6 Other Contributing Factors

Many other factors will play a critical role in determining the viability of materials-based storage in near-term markets including cost, cycle life/durability, reactivity, and effluent purity. Cost is an issue among all technologies. For materials-based hydrogen storage to be a practical alternative for near-term markets, the cost of the materials must be competitive with that of storage in high pressure cylinders. In addition, the hydrogen fuel cell system must be competitive with other forms of energy such as petroleum and diesel or batteries.

Compared to high pressure cylinders, materials-based hydrogen storage technologies have an inherent advantage since these materials can store hydrogen under moderate temperature and pressure.

In addition, specified impurities have been identified to cause significant reduction in fuel cell performance such as catalyst deactivation and degradation in membrane ionomer conductivity ultimately reducing the lifetime of the fuel cell (McWhorter *et al.*, 2011).

2.3 Hydrogen Storage Method

The hydrogen molecule (H_2) can be found in various forms depending on the temperature and the pressure. At low temperature hydrogen is solid with a density of 70.6 kg/m^3 at -262 °C and is a gas at higher temperature with density of 0.089886 kg/m^3 at 0 °C and a pressure of 1 bar and is a liquid hydrogen at -253 °C with a density of 70.8 kg/m^3. At ambient temperature (25 °C), hydrogen is a gas and can be described by the Van der Waals equation:

$$P(V) = \frac{nRT}{V-nb} - a \cdot \frac{n^2}{V^2} \tag{2.1}$$

where P is the gas pressure, V the volume, T the absolute temperature, n the number of moles, R the gas constant (R = 8.314 J/mol·K), a is the dipole interaction or repulsion constant ($a = 2.476\times10^{-2}$ m^6·Pa/mol^2), and b is the volume occupied by the hydrogen molecules ($b = 2.661\times10^{-5}$ m^3/mol). Hydrogen storage basically implies the reduction of the enormous volume of hydrogen gas; 1 kg of hydrogen at ambient temperature and atmospheric pressure takes a volume of 11 m^3. In order to increase the hydrogen density in a storage system, work must either be applied to compress hydrogen, or the temperature has to be decreased below the critical temperature, or finally, the repulsion has to be reduced by the interaction of hydrogen with another material. The second important criterion for hydrogen storage system is the reversibility of the hydrogen uptake and release. There are basically possible methods that can be used in order to reversibly store hydrogen with a high volumetric density and are shown in Table 2.2 (Züttel, 2004).

Table 2.2 Basic hydrogen storage methods and phenomena. The gravimetric density ρ_m, the volumetric density ρ_v the working temperature T and pressure P are listed. RT stands for room temperature (25 °C) (Züttel, 2004)

Storage method	ρ_m **(mass %)**	ρ_v **(kgH_2/m^3)**	T **(°C)**	P **(bar)**	**Phenomena and remarks**
High-pressure gas cylinders	13	<40	RT	800	Compressed gas (molecular H_2) in lightweight composite cylinder (tensile strength of the material is 2,000 MPa)
Liquid hydrogen in cryogenic tank	Size dependent	70.8	-252	1	Liquid hydrogen (molecular H_2), continuous loss of a few % per day of hydrogen at RT
Adsorbed hydrogen	≈ 2	20	-80	100	Physisorption on materials with a large surface specific area
Complex compound	<18	150	>100	1	Complex hydrides, desorption at elevated temperature, adsorption at high pressures

2.3.1 High Pressure Gas Cylinder

The most common storage system is high-pressure gas cylinders with a maximum pressure of 20 MPa. New lightweight composite cylinders have been developed, which are able to withstand a pressure up to 80 MPa and so the hydrogen can reach a volumetric density of 36 kg/m^3. The volume density of hydrogen increases with pressure and reaches a maximum above 100 MPa, depending on the tensile strength of the material. However, the gravimetric density decreases with increasing pressure and the maximum gravimetric density is found for zero overpressure. Therefore, the increase in volumetric storage density is sacrificed with the reduction of the gravimetric density in pressurized gas systems (Züttel, 2004).

The drawbacks of this method are high volume, high pressure, low density, and difficult to control pressure. Novel high pressure tanks made of carbon-fiber-reinforced composite material are being developed. Moreover, the cost and safety are still the key challenges for compressed hydrogen gas tanks (Satyapal *et al.*, 2007).

2.3.2 Liquid Hydrogen

Liquid hydrogen is stored in cryogenic tanks at -251.8 °C at ambient pressure. Due to the low critical temperature of hydrogen (-240 °C), liquid hydrogen can be stored in open systems, because there is no liquid phase existing above the critical temperature. The pressure in a closed storage system at room temperature could increase to about 10^4 bar. The volumetric density of liquid hydrogen is 70.8 kg/m^3 and slightly higher than that of solid hydrogen (70.6 kg/m^3) (Züttel, 2004).

However, the drawbacks are high cost for the liquefaction process (condensation temperature of hydrogen at 0.1 MPa and -252 °C) and heat transfer through the container leads to hydrogen loss (Satyapal *et al.*, 2007).

2.3.3 Chemical Hydrogen Storage

2.3.3.1 Hydrogenation/dehydrogenation Reaction

The hydrogenation and dehydrogenation of organic liquids (cyclic hydrocarbons or heteroaromatic compounds) offers a potential advantage by not requiring water on-board as co-reactant (Satyapal *et al.*, 2007). Aromatic compounds such as benzene, toluene, and naphthalene can be easily hydrogenated by using appropriate metal catalysts under relatively mild conditions, e.g. about 100 °C and 2 MPa. However, the dehydrogenation of cyclic hydrocarbons is highly endothermic and the reaction is favored only at high temperatures. One early example is the decalin-to-naphthalene reaction with platinum-based or other noble metal, which can release 7.3 wt% hydrogen at 210 °C.

The drawbacks of this method are still requiring relatively high temperatures for vaporization of the volatile components of the process and an important need is also an effective separation of hydrogen from the mixtures to get a pure hydrogen product and to reuse the hydrogen carrier materials (Zhao *et al.*, 2010).

2.3.3.2 Hydrolysis Reactions

Hydrolysis reactions involve the reaction of the chemical hydrides with water to produce hydrogen. The reaction of sodium borohydride solutions has been the most studied to date but borohydride production from borate requires multi-step conditions that are difficult on-board a vehicle and thus regeneration must take place off-board. Another hydrolysis reaction that is presently being investigated is the reaction of MgH_2 with water, to form $Mg(OH)_2$ and H_2. However, water must also be carried on-board the vehicle in addition to the slurry and the $Mg(OH)_2$ must be regenerated off-board. In all these cases, it cannot be assumed that water is available from the fuel cell subsystem at all operating conditions of the vehicle (Satyapal *et al.*, 2007).

2.3.3.3 Ammonia

Ammonia (NH_3), which has boiling point of -33.5 °C, has a high capacity for hydrogen storage, 17.6 wt%. However, in order to release hydrogen from ammonia (an endothermic reaction), high fuel processing temperature, and therefore large reactor mass and volume would be required. Moreover, the total system performance of on-board ammonia reactors (weight, volume start-up time, and etc.) would not meet the requirements for commercially viable hydrogen-powered fuel cell vehicles (Satyapal *et al.*, 2007).

2.3.4 Adsorption of Hydrogen

The adsorption of gas on a surface is a consequence of the field force at the surface of the solid, called the adsorbent, which attracts the molecules of the gas or vapour, called adsorbate. The original of the physisorption of the gas molecules on the surface of a solid are resonant fluctuations of the charge distributions and are therefore calling dispersive interactions or Van der Waals interactions. In the physisorption process, a gas molecule interacts with several atoms at the surface of the solid. The interaction is composed of two terms: an attractive term and a repulsive term. Due to the weak interaction, a significant physisorption is only observed at low temperature (< 0 °C). Once a monolayer of adsorbate molecules is formed, the gaseous molecules interact with the surface of the liquid or solid adsorbent. Therefore, the binding energy of the second layer of adsorbate molecules is similar to the latent heat of sublimation or vaporization of the adsorbate. Consequently, the adsorption of the adsorbate at a temperature equal to or greater than the boiling point at the given pressure leads to the adsorption of one single monomer (Züttel, 2004).

Nanostructure materials are a new class of materials with unique properties that stem from their reduced length scale (1 < d < 100 nm). The nanostructured materials considered for storing hydrogen are, for example, carbon nanostructure (carbon nanotubes, carbon nanofiber, and graphite nanofiber), and metal organic framework (MOF). Hydrogen can be stored by adsorbing (physisorption) on the surface of these materials (science.energy.gov).

Single-walled carbon nanotubes (SWNTs), and multi-walled carbon nanotubes (MWNTs), have been made since Dillon *et al.* (1997) first reported significant hydrogen adsorption of as prepared soot containing 0.1-0.2 wt% at 140 °C. Most recently, alkali-doped CNTs were found to adsorb only 2 wt% dry hydrogen at room temperature (Cho *et al.*, 2007).

MOFs are crystalline coordination polymers, which contain metal ions or clusters connected by organic linkers. A lot of research activities were focused on hydrogen in MOFs with most exiting results reported at cryogenic temperature (-196 °C). For instance, well-known and one of the most studied MOF-177 was reported to adsorb 6 wt% hydrogen at -196 °C and 6.6 MPa hydrogen pressure. At room temperature, the binding energy between hydrogen and MOFs is relatively weak and hydrogen uptake usually does not exceed 1 wt% (Luzan *et al.*, 2009).

Besides the carbon nanostructures, other nanoporous materials have been investigated for hydrogen adsorption. The hydrogen adsorption of zeolites of difference pore architecture and composition e.g. A, X, and Y was analyzed in the temperature range 20-300 °C and pressure range 2.5-10 MPa. The adsorbed amount of hydrogen increased with increasing temperature and increasing adsorption pressure. The absorbed amount of desorbed hydrogen was found to be 0.08 mass% for sample loaded at a temperature of 300 °C and a pressure of 10 MPa. At liquid nitrogen temperature (-196 °C), the zeolites physisorb hydrogen proportional to the specific surface area of the material. A maximum of 1.8 mass% of adsorbed hydrogen was found for a zeolite (NaY) (Züttel, 2004).

The major drawback of nanostructure materials is a very weak bond between hydrogen and adsorbent so hydrogen absorption can take place only in a cryogenic temperature. Moreover, a real value of hydrogen capacity by these materials is still contradicted, particularly for carbon nanotubes (science.energy.gov).

However, conducting polymer nanostructures can combine the advantages of organic conductors and low dimensional systems having interesting physicochemical properties and useful applications including for hydrogen storage and among the conducting polymers, polyaniline was considered important because of its extraordinary properties of electrical and optical behavior (Srinivasan *et al.*, 2010).

2.3.5 Metal Hydrides

Metals, intermetallic compound, and alloys generally react with hydrogen and form mainly solid metal-hydrogen compounds. Hydrides exist as ionic, polymeric covalent, and metallic hydrides. Metal hydrides are a chemical compound of hydrogen and metal at elevated temperatures (Züttel, 2004).

Metal hydrides can be divided into two types: transition metal hydrides and light weight metal hydrides. Light weight metal hydrides or alkali metal hydrides are divided into two parts: simple metal hydrides such as NaH, CaH_2, and

LiH, and complex metal hydrides are group I and II salts of $[AlH_4]^-$, $[NH_2]^-$, and $[BH_4]^-$ (alanates, amides, and borohydrides) such as $NaAlH_4$, $LiAlH_4$, and $LiBH_4$. Hydrogen is covalently bonded to the central atoms in complex anions (in contrast to interstitial hydrides) (Schüth *et al.*, 2004).

2.3.5.1 Improvement on Surface Properties and Mechanical Ball-Milling

A critical factor for hydrogen absorption by metals is the metal surface, which activates dissociation of hydrogen molecules and allows easy diffusion of hydrogen into the bulk. Diffusion is not the limiting step initially because no material has been reacted and there are sufficient active sites available, but chemisorption is the slowest step. As the reaction progresses, hydrogen diffusion takes place and the hydride layer grows, producing a nearly impermeable layer. Diffusion through this hydride layer becomes the rate-limiting step in the hydride formation process.

The ball-milling creating fresh surfaces during processing are an economic process that is widely applied to metal hydrides to achieve good surface properties. The main effects of ball-milling are increased surface area, formation of micro/nanostructures and creation of defects on the surface and in the interior of the material. The induced lattice defects may aid the diffusion of hydrogen in materials by providing many sites with low activation energy of diffusion. The induced microstrain assists diffusion by reducing the hysteresis of hydrogen absorption and desorption. The increased surface contact with catalyst during ball-milling leads to fast kinetics of hydrogen transformations. It is possible to control properties of the store material, according to specific applications (Sakintuna *et al.*, 2007).

2.3.5.2 Catalyst Effect

Catalysis is one of the critical factors in the improvement of hydrogen sorption kinetics in metal hydride systems that enable fast and effective dissociation of hydrogen molecules. Effective catalysts, even added in small amounts enhance the formation of a hydride in reasonable extent. There is intensive research about finding a proper catalyst to enhance the hydriding properties. It was reported that the rate of absorption is controlled by the following factors: the rate of hydrogen dissociation at the surface, the capability of hydrogen to penetrate from the surface which is typically covered by an oxide layer into metal, the rate of hydrogen diffusion into the bulk metal and through the hydride already formed (Sakintuna *et al.*, 2007).

However, metal hydrides are difficult to apply because they are too thermodynamically stable. This has two consequences. First, the hydrides have to be heated to an inconveniently high temperature to release hydrogen. Second, the heat of absorption is so high that a large amount of heat must be removed during the refueling process. In addition, the hydride systems contain strongly reducing agents which can react vigorously with air, and thus must be leakfree (Zhao *et al.*, 2010).

2.4 Hydrogen Storage in Polyaniline

Polyaniline (PANI) is a conducting polymer and most frequently studied because of its simple synthesis, environmental stability, and simple doping/dedoping chemistry. This versatility has made PANI attractive for numerous applications, including sensors, battery electrodes, display devices, anticorrosion coatings, field effect transistors, and potential hydrogen storage materials (Rahy *et al.*, 2011).

PANI can be synthesised by the oxidative polymerisation of aniline monomer in aqueous acidic media using a variety of oxidizing agents. It can be found in one of the three idealized oxidation states

- leucoemeraldine – white/clear & colorless
- emeraldine – green for the emeraldine salt, blue for the emeraldine base
- (per)nigraniline – blue/violet

The emeraldine form of PANI, often referred to as emeraldine base (EB), is neutral, if doped it is called emeraldine salt (ES), with the imine nitrogens protonated by an acid. Emeraldine base is regarded as the most useful form of PANI due to its high stability at room temperature and the fact that, upon doping with acid, the resulting emeraldine salt form of PANI is electrically conducting. Leucoemeraldine and pernigraniline are poor conductors, even when doped with an acid. The general structures of PANI are show in Figure 2.2.

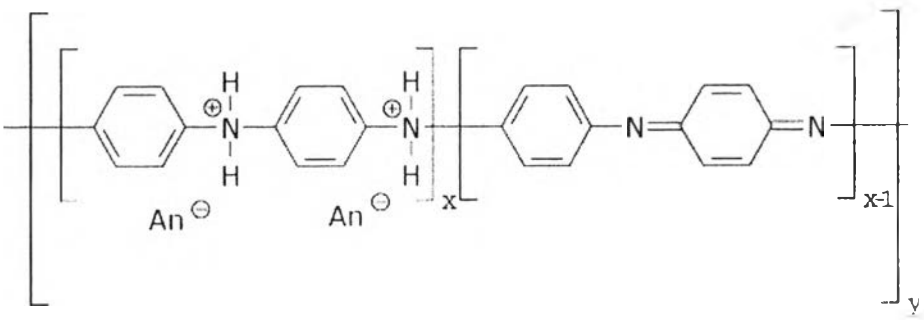

Figure 2.2 General structures of PANI conducting polymers (en.wikipedia.org/wiki/Polyaniline).

Important properties of PANI are its electric conductivity and can even have metallic properties. PANI is often called organic metal or organic nanometal Moreover, PANI has a great deal potential for applications due to their light weight, mechanical flexibility, and chemical properties. PANI is especially attractive because it is less expensive, has three distinct oxidation states with different colors, and has an acid/base doping response in the oxidation states. This latter property makes PANI an ideal option for acid/base chemical vapor sensors. The different colors, charges, and conformations of the multiple oxidation states also make the material highly promising for applications such as acutuators, supercapacitors, and printed circuit board (en.wikipedia.org/wiki/Polyaniline).

2.4.1 HCl-treated Polyaniline and Polypyrrole

Panella *et al.* (2005) investigated the volumetric measurement of hydrogen storage in HCl-treated PANI and polypyrrole (Ppy). PANI and Ppy were purchased from Sigma-Alderich Co. PANI was delivered as powder of emeraldine salt. Ppy was obtained from a 5 wt% solution in water, after evaporating the water, Ppy coated on polyurethane core resin with polymer/urethane ratio of 4. They were treated with HCl. Hydrogen storage was measured volumetrically with a Sievert's apparatus, in which the sample volume was determined from the pressure drop of the helium gas measured in the empty and filled sample chamber. The results show that no hydrogen storage was measured for HCl-treated PANI and Ppy, neither at room temperature nor at −196 °C.

Cho *et al.* (2007) conducted polymers in order to determine their potential as hydrogen storage media. The conducting polymers, PANI and Ppy, were purchased from Sigma-Aldrich and were treated with an acid. The hydrogen sorption capacity was measured using an automatic Sievert's type PCT measurement apparatus. The level of hydrogen sorption on the Ppy and the PANI was measured after evacuation at 25 °C for 1 h, reaching about 3.5 wt% hydrogen. The sample was then evacuated at 200 °C to remove the adsorbed hydrogen, the level of sorption increased to about 6.4 wt%. The effect of the HCl treatment on the conducting polymer was observed as a change in the surface structure, and it might induce the formation of micropores or micro-leaks that are desirable for hydrogen sorption.

2.4.2 Polyaniline Nanocomposite

Jurczyk *et al.* (2007) reported the use of PANI for hydrogen storage. The conducting polymer-based nanocomposite was modified to increase the porous structure of the nanocomposite and the number of binding sites, which, in turn, enhanced the hydrogen storage capacity. PANI was synthesized by following a well-established method for the synthesis of the emeraldine base (EB), a form of PANI, and was modified with filler materials such as multiwall carbon nanotubes, tin oxide (SnO_2), and fine aluminum powder. The isothermal volumetric measurements were carried out by Sievert's type PCT sorption equipment. The standard PANI was capable of storing 0.35 wt% hydrogen at 125 °C. When SnO_2 was added, no change in the hydrogen sorption capabilities was obtained. Similarly, the multiwall carbon nanotubes showed no effect on the hydrogen capabilities of the material. For the hydrogen sorption performed on the PANI with aluminum powder, it exhibited a much higher hydrogen sorption than the other samples. The increase in the hydrogen sorption capabilities caused by the inclusion of fine aluminum powder, as well as the exact chemical interaction between the aluminum and the PANI, is still being investigated.

Kim *et al.* (2010) studied the enhancement of hydrogen storage capacity in polyaniline vanadium pentoxide nanocomposites (PANI-VONC). The high-pressure hydrogen sorption isotherms of PANI–VONC have been performed at liquid nitrogen temperature (-196 °C), and were measured volumetrically with pressure-composition isotherm (PCT) measurement. Hydrogen storage capacity in PANI–VONC was 1.8 wt% in contrast to that in pristine vanadium pentoxide (VO) (0.16 wt %) and in non-treated PANI (0.15 wt%). It revealed that the VO and PANI adsorb a small amount of hydrogen. However, the hydrogen storage capacity was enhanced in the PANI–VONC nanosheets. A reason for the enhancement of hydrogen storage was the intercalation of PANI into the VO layers and decreases in the interlayer distance from 1.1 nm between VO layers to 0.72 nm between VO layer and PANI layer.

2.4.3 Polyaniline Fibers

Srinivasan *et al.* (2010) investigated the reversible hydrogen storage in electrospun polyaniline fibers. PANI was produced via traditional chemical synthesis methods and then electrospun to produce fibers and the volumetric hydrogen sorption was carried out by PCT measurement. Hydrogen sorption capacity increased with increasing temperature from 50 to 125 °C in various cycles at a high pressure (about 8 MPa). At 100–125 °C, an increase in the capacity (6–8 wt%) was obtained. At the end of adsorption PCT, desorption PCT experiments were performed, and the hydrogen storage capacity of 2–8 wt% was obtained in a temperature range of 50–125 °C. The surface morphologies before and after hydrogen sorption on PANI fibers encompassed significant changes in the microstructure (nanofibrallar swelling effect), which probably leads to higher volumetric hydrogen storage capacity.

Rahy *et al.* (2011) reported a facile and environmentally friendly synthesis of polar solvent soluble polyaniline nanofibers by oxidative polymerization of aniline in the presence of organic additive such as sucrose, $C_{11}H_{22}O_{11}$ or sucralose, $C_{12}H_{19}C_{13}O_8$. For hydrogen sorption measurement, the PCT adsorption apparatus was employed to measure the hydrogen adsorption at 25 °C after removing adsorbed impurities of the sample. The solubilization of PANI synthesized with sucrose or sucralose was studied by dissolving PANI with water and other organic solvent. When PANI synthesized in the absence of sucrose was used, no solubilization occurred so, sucrose facilitates PANI to be dissolved and stabilized in water and polar solvent. In addition, PANI synthesized using sucrose and KIO_3/bleach as oxidant can adsorb hydrogen in the range of 3.7-4.3 wt% at 25 °C and 20 atm. The reasons why PANI nanofibers synthesized in the presence of sucrose can adsorb hydrogen are possibly due to sucrose can create nano-pores as the hypercrosslinked PANI produced to make the fibers have hydrogen absorption capability.

2.5 Hydrogen Storage in Polymeric Foam

Polymer foams are made up of a solid and gas phase mixed together to form a foam, they can be divided into either thermoplastics or thermosets, which are further divided into rigid or flexible foams. Widely known polymeric foams are polyurethane and polystyrene (Sivertsen, 2007).

Banyay *et al.* (2007) examined advancement in polymer and composite foam technologies for hydrogen storage because polymeric foams are a potential practical method of on-board vehicle hydrogen storage. Cross-linked PVC foam and elastomeric polyurethane foam were chosen. The polymeric foam has a much lower density, more conformable, and hydrogen permeable than metal foam thus making polymeric foam the desired choice over metallic foam.

Pientka *et al.* (2009) studied the application possibilities of polystyrene foams, and the experiments have proven that closed cell polymeric foams are able not only to separate and storage hydrogen but even to absorb of hydrogen. For hydrogen storage, closed cell polymeric foams can be utilized as a hydrogen container. Each cell serves as a small pressure vessel, which is filled through its wall. Important feature of the container is the forces generated by pressurized gas are compensated by foam structure. It is a new safe approach in comparison to traditional pressure vessels.

2.6 Hydrogen Storage by Hydrogenation/Dehydrogenation Reaction

Hydrogen storage in form of liquid organic hydrides employs hydrogenation-dehydrogenation of cyclic hydrocarbons or heteroaromatic compounds as a means to store and transport hydrogen. Aromatic compounds such as benzene, toluene, naphthalene, and 9-ethylcarbazole can be easily hydrogenated by using appropriate metal catalysts (catalytic hydrogenation) under liquid- film state condition, where the reactant is supplied as a liquid so that the surface of the catalyst is always wetted with a thin film (Zhao *et al.*, 2010).

2.6.1 Decalin Dehydrogenation/Naphthalene Hydrogenation

Hodoshima *et al.* (2003) proposed a catalytic decalin dehydrogenation/ naphthalene hydrogenation pair as a hydrogen source for fuel-cell vehicles. Catalytic hydrogen evolution from various amounts of added decalin and a carbon-supported platinum catalyst was performed under the mild conditions in a batch-wise catalytic dehydrogenation reactor to investigate the storage densities of hydrogen on both weight and volume bases. The highest conversion of decalin (41.1%) and the highest initial rate of hydrogen evolution (60.0 mmol/h) were attained by adopting this liquid-film type catalysis. The increased heating temperature from 210 to 280 °C enhanced the hydrogen evolution rates, and the decalin conversions higher than 95% were attained within 1.5 h at the heating temperature at 280 °C, and the rate of hydrogen evolution was as high as 400.0 mmol/h.

Sebastián *et al.* (2008) investigated the different platinum catalysts supported on activated carbon for decalin dehydrogenation under reactive distillation conditions and operate with the batch-type system. The volume of hydrogen released during the reaction was monitored by the water volume displaced in a buret, and decalin conversions were obtained on the basis of evolved hydrogen after stoichiometric confirmation of the naphthalene concentration in the reaction solution from gas chromatographic analyses. From dehydrogenation experiments, the reaction rate constant increased with temperature (conducting experiment at 260 °C), the maximum final decalin conversion obtained was about 60%, the optimum Pt loading in activated carbon for catalysts up to 4 wt% Pt and the optimum decalin/catalyst ratio was about 2.7 ml/g.

2.6.2 Reversible Catalytic Hydrogenation/Dehydrogenation of Terphenyl

Sung *et al.* (2008) studied the noble metal catalysts for a reversible hydrogen storage system. The noble metal catalysts on mesoporous SiO_2 and modified carbon supports were found to enhance the activities of terphenyl (TPh) hydrogenation and tercyclohexane (TCH) dehydrogenation without side reactions. Hydrogenation was monitored by the hydrogen pressure in the autoclave and the hydrogen consumption (ΔP) was converted into the volume of reacted hydrogen or the hydrogen storage capacity considering hydrogen loaded to TPh (wt%). The hydrogenation reaction temperature was heated up to 160 °C, and the dehydrogenation reaction temperature was heated up to 310 °C. A good hydrogenation/dehydrogenation was achieved over the 5% Pt/SiO_2 catalyst without stirring but from XPS and EXAFS analyses of the catalysts showed that the agglomeration of metal particles on the support was much less for the Pt catalyst. Therefore, 10% Pt/C catalysts are preferable to cycling of hydrogenation/dehydrogenation in a hydrogen storage system and stirring is necessary to provide a more rapid reversibility in TPh hydrogenation and TCH dehydrogenation.

2.6.3 Hydrogenation of 2-Methylthiophene

Zhao *et al.* (2010) investigated alkyl substituted thiophenes as candidates for hydrogen carriers. Four types of catalysts were investigated for 2-methylthiophene (2MT) hydrogenation and ring-opening. Hydrogenation activity was measured in a continuous-flow trickle bed reactor at 2 MPa, and the reactivity testing was carried out as a function of temperature, which was started at the highest temperature 325 °C and was varied downwards and upwards. The major products of hydrogenation reaction were tetrahydro-2-methylthiophene (TH2MT), pentenes, and pentane. The selectivity towards the desired product TH2MT follows the order: noble metals > bimetallics > phosphides > sulfides and the best hydrogenation catalyst was 2% Pt/Al_2O_3, which exhibited relatively high reactivity and selectivity towards TH2MT at moderate temperatures.

2.6.4 Hydrogenation of 9-Ethylcarbozole

Ye *et al.* (2011) studied the hydrogenation kinetics of 9-ethylcarbazole over Raney-Ni catalyst by investigating the influences of the reaction temperature, pressure, and catalyst concentration on the mass transfer-reaction processes. The reactions were conducted in an autoclave with magnetic stirring and the quantity of the consumed hydrogen was recorded by the pressure gauge, and the reaction time was measured. The whole reaction process was controlled by the surface reaction of the catalyst particles due to the increasing of the Raney-Ni catalyst dosage. The reaction rate gradually increased and the hydrogen absorption capacity was raised from 1.85 wt% to 4.92 wt%, and the maximum hydrogen capacity was about 5.0 wt% at 180 °C and 6 MPa.

2.7 Hydrogen Storage in Metal-Organic Frameworks (MOFs)

A new class of porous metal-organic frameworks (MOFs) has attracted much attention for hydrogen storage because of their exceptionally high specific surface area and microporosity, uniform but tunable pore size, very low density, and well-defined hydrogen occupation sites. A variety of linker molecules of MOFs can be used to create an entire family of materials having different pore sizes and containing different chemical functionalities within the linkers (Hu *et al.*, 2011).

Hydrogen adsorption properties of some Co-and Zn-based MOFs materials were studied at near ambient temperatures for hydrogen storage (Luzan *et al.*, 2009). Zn- and Co-based MOFs with different pore structures were synthesized. Two topological isomer of [$Zn_2(bcd)_2(dabco)$], which were ZBDt (have a square-grid net topology (square channels)) and ZBDh (consisted of triangle and hexagonal channels (pillared Kagome net)), were obtained. Hydrogen adsorption was measured by gravimetric method using a magnetic suspension balance from Rubotherm using hydrogen pressure up to 18 MPa and temperature interval of 20 to 100 °C. The highest hydrogen uptake equal to 0.51 wt% was observed for ZBDh at 20 °C and 120 bar. ZBDt was found to be slightly smaller, which was 0.42 wt%. These hydrogen uptake were found to depend linearly on the BET specific area and to depend strong on temperature. In addition, the hydrogen adsorption in MOFs caused by physisorption and the difference in the hydrogen adsorption capacity could possibly originate from partial collapse of structure in the treatments for removal of solvent traces and complete degassing.

2.8 Hydrogen Storage in Several Microporous Zeolites

Zeolites are a family of highly crystalline aluminosilicate materials. Abounding with cage and channel structures, high thermal stability, and large ion-exchange capacity, they offer enormous potential for the encapsulation of nonpolar gases. The mechanism of adsorption in zeolites is that hydrogen molecules are forced into the cavities under pressure and low temperature (Dong *et al.*, 2007).

Dong *et al.* (2007) investigated hydrogen storage in several microporous zeolites with different surface area, channel diameters, and pore volume such as Na-LEV, H-OFF, Na-MAZ, and Li-ABW, which were synthesized by different methods. The hydrogen uptake isotherms were measured by a commercial PCT method at liquid nitrogen temperature. Zeolite Na-LEV, which has appropriate channel diameter and a large pore volume, had the largest hydrogen storage of 2.07 wt% under 1.6MPa. Under the same condition, the hydrogen storage capacities of zeolites H-OFF and Na-MAZ were intermediate, 1.75 and 1.64 wt%, respectively, and zeolite Li-ABW presented the least hydrogen storage (1.02 wt%), because it only has a channel framework. The important parameters affecting hydrogen storage capacity is an optimal channel diameter, large cage volume at low temperature, and high pressure. The most effective channel size of zeolites was found to be near the kinetic diameter of a hydrogen molecule.

2.9 Hydrogen Storage in Metal Nitrides

Complex hydrides composed of light elements such as Li and Na have recently attracted great attention as hydrogen storage materials, because their gravimetric hydrogen densities are higher than those of conventional metal hydride systems.

The hydrogen storage properties of lithium nitride Li_3N is generally accepted that the hydrogenation and dehydrogenation of Li_3N proceed by the following 2-step reversible reactions (Palumbo *et al.*, 2008):

$$Li_3N + 2H_2 \leftrightarrow 2Li_2NH + LiH + H_2 \qquad (2.2)$$

$$Li_2NH + LiH + H_2 \leftrightarrow 2LiNH_2 + 2LiH \qquad (2.3)$$

Kojima *et al.* (2006) investigated hydrogen storage of metal nitrides by a mechanical reaction that was performed in a planetary ball mill in a hydrogen atmosphere at a pressure of 1 MPa and room temperature. Metal nitrides that were studied consist of Li_3N, Ca_3N_2, h-BN, Mg_3N_2, Si_3N_4, AlN, TiN, VN, and ZrN. Hydrogen absorption properties of the metal nitrides were measured with PCT measurement, automatic measuring system (Sievert's type apparatus). The ball-milled light metal nitrides such as Li_3N and Ca_3N_2 have the hydrogen contents above 3 wt%, whereas the other metal nitrides can store hydrogen less than 2 wt%.

2.10 Hydrogen Storage in Metal Hydrides

Hydrogen forms metal hydrides with some metals and alloys leading to solid-state storage under moderate temperature and pressure. There are two possible ways of hydriding a metal, direct dissociative chemisorption and electrochemical splitting of water. These reactions are:

$$M + \frac{x}{2}H_2 \leftrightarrow MH_x \qquad (2.4)$$

$$M + \frac{x}{2}H_2O + \frac{x}{2}e^- \leftrightarrow MH_x + \frac{x}{2}OH^- \qquad (2.5)$$

where M represents the metal.

Metal hydrides compose of metal atoms that constitute a host lattice and hydrogen atoms. Metal and hydrogen usually form two different kinds of hydrides, α-phase at which only some hydrogen is absorbed and β-phase at which hydride is fully formed. Hydrogen storage in metal hydrides depends on different parameters and consists of several mechanistic steps. Metals differ in the ability to dissociate hydrogen, this ability being dependent on surface structure, morphology and purity.

An optimum hydrogen-storage material is required to have the following properties; high hydrogen capacity per unit mass and unit volume which determines the amount of available energy, low dissociation temperature, moderate dissociation pressure, low heat of formation in order to minimize the energy necessary for hydrogen release, low heat dissipation during the exothermic hydride formation, reversibility, limited energy loss during charge and discharge of hydrogen, fast kinetics, high stability against O_2 and moisture for long cycle life, cyclibility, low cost of recycling and charging infrastructures, and high safety.

The light metals such as Li, Be, Na, Mg, B and Al, form a large variety of metal–hydrogen compounds. They are especially interesting due to their light weight and the number of hydrogen atoms per metal atom, which is in many cases at the order of $H/M = 2$. Heavier ones may enter the multiple component system only as a low abundant additive, most likely for alteration of properties or as a catalyst (Sakintuna *et al.*, 2007).

Lithium alanate or lithium aluminum hydride ($LiAlH_4$) has high hydrogen capacity for complete decomposition (7.9 wt%). It has multiple steps for decomposition

$$3LiAlH_4 \rightarrow Li_3AlH_6 + 2Al + 3H_2 \qquad (2.6)$$

$$Li_3AlH_6 \rightarrow 3LiH + Al + \frac{3}{2}H_2 \qquad (2.7)$$

The first step, eq. (2.6), takes place at 160 °C and releases 5.3 wt% hydrogen. The second step, eq. (2.7), releases 2.6 wt% hydrogen and occurs at about 200 °C. The unreleased part as LiH can be decomposed at a very high temperature, above 680 °C (Zaluski *et al.*, 1999).

Xueping and Shenglin (2009) studied the hydrogen storage properties of $LiAlH_4$ by doping with 5 mol% Ti, Ni, $Ce(SO_4)_2$, and $LaCl_3$ by using ball milling. All the doped samples had lower desorption temperature and rate of hydrogen released in the first stage than the undoped one. Doping with $Ce(SO_4)_2$ decreased the desorption temperature by 38 °C compared with as-received $LiAlH_4$. In addition, the amount of hydrogen released was decreased by doping with Ti and $LaCl_3$. For absorption, doping with Ti showed the most promising results under 8 MPa at 180 °C for 2 h.

The effect of additives on the reversibility of $LiAlH_4$ was investigated by Xueping and Shenglin (2009). Doping with 1 mol% Ti, Ni, Fe, and $Ce(SO_4)_2$ decreased the desorption temperature except doping with $LaCl_3$. The addition of Fe markedly decreased the hydrogen desorption temperature, 37 °C, while the amount of hydrogen released had decreased. Furthermore, the rate of hydrogen released was decreased regardless on dopants. $LiAlH_4$ doped with 1 mol% Ni exhibited the highest hydrogen absorption about 0.97 wt% at 180 °C under 8 MPa for 2 h.

Léon *et al.* (2009) investigated alanate mixtures ($LiAlH_4$+MgH_2) produced by reactive ball milling. They found that a milling speed and milling time were important parameters to the new hydride phase formation. For the sample ball-milled at 600 rpm, one or two new phases were observed, which showed the fast desorption kinetics. At 300 °C under 0.5 bar H_2, alanate mixtures released about 6.5 wt% hydrogen within 2,000 s during first cycle desorption, while only 2.5 wt% H_2 were released within 3,500 s during the second cycle desorption indicating that only MgH_2 was formed after the hydrogen uptake.

Li *et al.* (2007) investigated effects of ball milling and additives on dehydrides of well-cryatallized $Mg(BH_4)_2$. $Mg(BH_4)_2$ was chemically synthesized in diethyl ether according to this reaction:

$$2NaBH_4 + MgCl_2 \rightarrow Mg(BH_4)_2 + 2NaCl \qquad (2.8)$$

Powers of $TiCl_3$, TiO_2, TiB_2, TiH_2, and Ti were added to the as-synthesized $Mg(BH_4)_2$ in a weight ratio of 1:3 by ball milling for 2 h. The dehydriding reaction initiates at about 262 °C and a weight loss of approximately 13.7 mass% is confirmed up to 527 °C. For DTA curves shows two endothermic peaks at approximately 301 °C and 372 °C. The hydrogen desorption reaction of $Mg(BH_4)_2$ has been investigated and the results indicate that hydrogen is desorbed in the following two steps:

$$Mg(BH_4)_2 \rightarrow MgH_2 + 2B + 3H_2 \rightarrow Mg + 2B + 4H_2 \qquad (2.9)$$

For the XRD profiles of $Mg(BH_4)_2$ milled for 2 and 5 h, the diffraction peaks almost disappear and are replaced by a broad maximum even after 2 h of ball milling, suggesting that an amorphization reaction is induced by the ball milling and indicated that the dehydriding reaction is hardly affected by the ball milling. For the effect of catalyst, the initial dehydriding temperature is reduced by the addition of $TiCl_3$.

Matsunaga *et al.* (2008b) synthesized $Mg(BH_4)_2$ by decomposition reaction of $LiBH_4$ with $MgCl_2$ by heat treatment without using a solvent for hydrogen storage. The reaction during the first heating procedure is assumed as:

$$2LiBH_4 + MgCl_2 \rightarrow Mg(BH_4)_2 + 2LiCl \qquad (2.10)$$

For TPD measurement, the sample after heat treatment (at the temperature > 250 °C at 10MPa of hydrogen) has two desorption peaks, it start to decompose at 227 °C and the first desorption peak appear around 290 °C and the second desorption peak starts at 327 °C. The shape of two independent desorption peaks implies that decomposition reaction consists of two steps and the product consists of LiCl and a compound of magmesium, boron, and hydrogen. This result indicated that $Mg(BH_4)_2$ has two step reaction

$$Mg(BH_4)_2 \rightarrow MgH_2 + 2B + 3H_2 \qquad (1^{st}\ \text{step}) \qquad (2.11)$$

$$MgH_2 \rightarrow Mg + H_2 \qquad (2^{nd}\ \text{step}) \qquad (2.12)$$

From the Van't Hoff plot obtained by equilibrium pressures of the first decomposition varied from 1.4 MPa at 290 °C to 3.1 MPa at 350 °C, the dehydrogenation enthalpy of the first decomposition is found to be $\Delta H = -39.3$ kJ/mol H_2. However, only the second reaction step ($MgH_2 \rightarrow Mg$) is reversible at the condition up to 350 °C at 10 MPa of hydrogen.

Soloveichik *et al.* (2009a) investigated different methods for preparation of unsolvated magnesium borohydride, based on exchange reaction of $MgCl_2$ with lithium and sodium borohydride in different solvents have been evaluated. The different methods are consist of (1) reaction of $LiBH_4$ with $MgCl_2$ in diethyl ether, (2) reaction of $NaBH_4$ with $MgCl_2$ in diethyl ether, these both reactions were followed by desolvation $Mg(BH_4)_2$ solvates and the last one is reaction of $MgCl_2$ with $NaBH_4$ in amines. The results from XRD, IR spectra, and TGA, can conclude that only reaction of $NaBH_4$ with $MgCl_2$ in diethyl ether is the method most suited for mass production. Because the reaction of $LiBH_4$ with $MgCl_2$ in ether gives $Mg(BH_4)_2$ contaminated with lithium and chlorine due to formation of ternary complexes like $NaBH_4$ with $MgCl_2$ in amines also yield contaminated products.

Another report from Soloveichik *et al.* (2009b) they studied properties and dehydrogenation pathway of unsolvated $Mg(BH_4)_2$. From TPD curve, it show at least four steps for decomposition of $Mg(BH_4)_2$ with the maximum release rate at 295 °C (1st step) and 325 °C (2nd step). About 4.7% hydrogen is evolved in 1st step and another 4.9% is released in 2nd step, for a total about 9.6%. A third smaller decomposition step is observed with onset at 395 °C and maximum release rate at 410 °C and produces 3.3–3.7% hydrogen. The decomposition products may be compose of several polyborane intermediate species and includes an exothermic reaction yielding crystalline MgH_2 as an intermediate and these products may be only partially recharged after the very first step and also via hydrogenation of Mg metal.

Zhang *et al.* (2010) studied direct synthesis of $Mg(BH_4)_2$ by mechanical milling of pure Mg–B powder and then a hydrogenation process under a hydrogen atmosphere. Commercial Mg powder with a purity of 99.9% and amorphous B powder with a purity of 99% were mixed as the raw milling materials and vary many factors such as weight ratio of ball to powder, weight ratio of big balls to small balls, working time versus rest time, and milling speed. From XRD patterns, it can be concluded that no other phase such as the solid solution of Mg or MgB_2 phase was formed during the milling process. Hydrogenation properties of Mg–B powders in a hydrogen atmosphere were examined at 300 °C using a PCT measurement and the reduction of crystallite size showed a more obvious effect on improving the absorption kinetic properties than that of the particle size. However, no successful synthesis of $Mg(BH_4)_2$ was achieved. The obtained nanocrystalline hydride was MgH_2. It was found that the addition of B into magnesium strongly enhanced the kinetic properties of magnesium hydrogenation.

Pistidda *et al.* (2010) reported synthesis of amorphous $Mg(BH_4)_2$ from MgB_2 and H_2 at room temperature. The starting materials were milled in planetary mill at rotation speed of 600 rpm for up to 100 h and subsequently a hydrogen pressure of 100 bar was applied. From *in situ* XRD measurement, it confirmed the amorphous state of the material and showed the typical crystalline decomposition products of $Mg(BH_4)_2$ at elevated temperatures. Furthermore, solid-state NMR showing the characteristic features of $Mg(BH_4)_2$ and other $Mg(B_nH_m)_y$ species. Therefore, amorphous $Mg(BH_4)_2$ can be synthesized by solid–gas reaction with a yield of approximately 50% from MgB_2 and hydrogen by high pressure ball milling.

Zhang *et al.* (2011) investigated synthesis $Mg(BH_4)_2$ by mechanically milling Mg + B, MgH_2 + B and MgB_2 powders following hydrogenation under hydrogen atmosphere. The XRD pattern of the milled Mg + B powders demonstrates the coexistence of magnesium hydride and boron, which indicates the reaction of $Mg + H_2 \rightarrow MgH_2$ during the milling process under n hydrogen atmosphere. For the milled MgH_2 + B powder, the XRD shows little difference in comparison to the Mg + B powders. It seems that the MgH_2 did not readily react with boron even using high energy milling under high hydrogen pressure. From the XRD pattern of the milled MgB_2 powder, MgB_2 appears to be quite stable during the milling process. These results indicate the difficulty of breaking the B-B bonds throughout the reaction of boron and hydrogen, because both pure boron and MgB_2 contain stable boron bonds. Furthermore TPD measurements confirmed the formation of amorphous Mg-B-H compounds, which could be $Mg(B_xH_y)_n$ moieties. The total amount of hydrogen desorption of the milled Mg + B and MgH_2 + B powders after 3 h was 3.7 wt.% and 3.9 wt.%, respectively, while the milled MgB_2 showed little apparent hydrogen desorption. After further hydrogenation carried out under 12 MPa hydrogen pressure at 450 °C and for 120 h, the Mg + B powder demonstrated MgH_2 grain growth, while the existence of amorphous Mg-B-H compounds in the MgB_2 powder was confirmed by Raman spectral analysis. The hydrogenated MgB_2 powder also released 0.25 wt.% hydrogen. It was suggested that use of a metal to form a metal boride as a precursor may be an effective way to enhance the hydrogen absorption kinetics thereby the formation of borohydrides.